

Quantifying spin contamination in algebraic diagrammatic construction theory of electronic excitations

Terrence L. Stahl¹ and Alexander Yu. Sokolov^{1, a)}

*Department of Chemistry and Biochemistry, The Ohio State University, Columbus, Ohio 43210,
USA*

Algebraic diagrammatic construction (ADC) is a computationally efficient approach for simulating excited electronic states, absorption spectra, and electron correlation. Due to their origin in perturbation theory, the single-reference ADC methods may be susceptible to spin contamination when applied to molecules with unpaired electrons. In this work, we develop an approach to quantify spin contamination in the ADC calculations of electronic excitations and apply it to a variety of open-shell molecules starting with either the unrestricted (UHF) or restricted open-shell (ROHF) Hartree–Fock reference wavefunctions. Our results show that the accuracy of low-order ADC approximations (ADC(2), ADC(3)) significantly decreases when the UHF reference spin contamination exceeds 0.05 a.u. Such strongly spin-contaminated molecules exhibit severe excited-state spin symmetry breaking that contributes to decreasing the quality of computed excitation energies and oscillator strengths. In a case study of phenyl radical, we demonstrate that spin contamination can significantly affect the simulated UV/Vis spectra, altering the relative energies, intensities, and order of electronic transitions. The results presented here motivate the development of spin-adapted ADC methods for open-shell molecules.

I. INTRODUCTION

Molecules with unpaired electrons are the key intermediates in a variety of chemical processes that are important in environmental and combustion chemistry, organic synthesis, catalysis, and biochemistry.^{1–15} A powerful tool to identify the presence of these short-lived chemical species is the UV/Vis absorption spectroscopy, which combines high sensitivity and specificity, allowing to detect transient species in low concentrations. However, compared to stable closed-shell molecules, the UV/Vis spectra of molecular radicals are much less understood and can be difficult to interpret without the insight from accurate theoretical calculations.

Meanwhile, simulating UV/Vis spectra of open-shell molecules is often challenging as they tend to exhibit complicated ground- or excited-state electronic structures, which require rigorous treatments of electron correlation, spin, and orbital relaxation. Open-shell electronic states can be accurately described using non-perturbative theoretical approaches, such as configuration interaction,^{16–25} coupled cluster theory,^{26–34} orbital-optimized methods,^{35–42} and multireference techniques.^{43–59} However, the computational cost of these methodologies scales steeply with the number of electrons and orbitals in a molecule, significantly constraining their applications. Lower-cost single-reference approaches for simulating UV/Vis spectra of open-shell molecules have been also developed, but their accuracy strongly depends on the quality of Hartree–Fock (HF) reference wavefunction that is employed as the zeroth-order approximation.

Of particular concern is the unphysical violation of spin symmetry, known as spin contamination,^{60–66} which is frequently encountered in the unrestricted HF (UHF) calculations of open-shell ground-state wavefunctions and is even more common for excited states. Spin contamination can give rise to large errors in computed excitation energies, unphysical transition intensities, and incorrect description of state crossings, leading to inaccurate UV/Vis spectra. Although spin contamination is inherent in open-shell calculations using most single-reference methods, it is particularly detrimental for post-HF approaches based on low-order perturbation theory.

In this work, we investigate spin contamination in the calculations of excited states and UV/Vis spectra of open-shell molecules using algebraic diagrammatic construction theory (ADC).^{67–74} ADC obtains excitation energies and transition intensities by perturbatively approximating the poles and residues of the polarization propagator and is one of the most widely used theoretical approaches for calculating excited states. In particular, the second-order ADC method (ADC(2)) has been extensively used for calculating the UV/Vis spectra of large molecules^{75–85} due to its relatively low $\mathcal{O}(M^5)$ computational scaling with the basis set size M and ability to incorporate electron correlation effects. More accurate and expensive ADC(3)^{71,77,86–88} and ADC(4)⁸⁹ approximations have been also developed.

Although the performance of low-order ADC methods for open-shell molecules has been studied,^{75,90,91} it is yet unclear how significant is spin contamination (SC) in its calculations when starting from the unrestricted (UHF) or restricted open-shell HF (ROHF) reference wavefunctions. Does the extent of SC in UHF reference wavefunction correlate with the magnitude of SC in excited states computed using ADC? Is it possible to reduce the excited-state SC in ADC calculations by starting with the ROHF reference wavefunction? Does SC reduce with

^{a)}Electronic mail: sokolov.8@osu.edu

increasing order of ADC approximation? And, does it affect the accuracy of ADC oscillator strengths and UV/Vis spectra? Here, we aim to answer these questions by implementing the calculation of spin operator expectation values in ADC methods and quantifying the SC in neutral excited states of small open-shell molecules. This work is a continuation of our earlier study where we investigated the SC in ADC calculations of charged excitations.⁹²

This paper is organized as follows. First, we review ADC for the polarization propagator and describe an approach for calculating spin expectation values and contamination (Section II). Next, following the description of our implementation and computational details (Section III), we present and discuss our calculations of SC in small open-shell molecules, correlating the errors in spin expectation values with the errors in computed excitation energies (Section IV A) and oscillator strengths (Section IV B). Finally, in Section IV C, we carry out a study of phenyl radical UV/Vis spectrum where we analyze the effect of SC on the energies and intensities of individual electronic transitions.

II. THEORY

A. Algebraic diagrammatic construction for the polarization propagator

The electronic excitations in linear UV/Vis spectroscopy are characterized by the polarization propagator^{93–96}

$$\begin{aligned} \Pi_{pq,rs}(\omega) &= \sum_{n \neq 0} \frac{\langle \Psi_0^N | a_q^\dagger a_p | \Psi_n^N \rangle \langle \Psi_n^N | a_r^\dagger a_s | \Psi_0^N \rangle}{\omega + E_0^N - E_n^N} \\ &+ \sum_{n \neq 0} \frac{\langle \Psi_0^N | a_r^\dagger a_s | \Psi_n^N \rangle \langle \Psi_n^N | a_q^\dagger a_p | \Psi_0^N \rangle}{-\omega + E_0^N - E_n^N} \\ &= \Pi_{pq,rs}^+(\omega) + \Pi_{qp,sr}^-(\omega) \end{aligned} \quad (1)$$

that describes how the N -electron chemical system in state $|\Psi_0^N\rangle$ with energy E_0^N (usually, the ground state) interacts with a periodic electric field with frequency ω . In Eq. (1), the two components of $\Pi_{pq,rs}(\omega)$, known as the forward ($\Pi_{pq,rs}^+(\omega)$) and backward ($\Pi_{qp,sr}^-(\omega)$) polarization propagators, are expressed in terms of the exact wavefunctions ($|\Psi_n^N\rangle$) and energies (E_n^N) of all electronic states. In this so-called spectral (or Lehmann) representation, each contribution to $\Pi_{pq,rs}(\omega)$ can be written more compactly as

$$\mathbf{\Pi}^\pm(\omega) = \tilde{\mathbf{X}}^\pm(\omega \mathbf{1} - \tilde{\Omega}^\pm)^{-1} \tilde{\mathbf{X}}^{\pm\dagger} \quad (2)$$

where $\tilde{\mathbf{X}}^\pm$ are the matrices of spectroscopic amplitudes ($\tilde{X}_{pq,n}^\pm = \langle \Psi_0^N | a_q^\dagger a_p | \Psi_n^N \rangle$, $\tilde{X}_{rs,n}^- = \langle \Psi_0^N | a_r^\dagger a_s | \Psi_n^N \rangle$) describing the probability of electronic transitions between two molecular orbitals and $\tilde{\Omega}^\pm$ is the diagonal matrix of transition energies with elements $\tilde{\Omega}_n^\pm = E_n^N - E_0^N$ or

$$\tilde{\Omega}_n^- = -E_n^N + E_0^N.$$

In algebraic diagrammatic construction (ADC),^{67–74,96} the excitation energies and transition probabilities in UV/Vis spectra are computed by approximating $\tilde{\mathbf{X}}^\pm$ and $\tilde{\Omega}^\pm$ using perturbation theory. These approximations are derived by ensuring that at any perturbation order $\mathbf{\Pi}^+(\omega)$ and $\mathbf{\Pi}^-(\omega)$ are fully decoupled from each other and can be treated independently. Due to the time-reversal symmetry, the backward polarization propagator can be obtained as $\mathbf{\Pi}^-(\omega) = (\mathbf{\Pi}^+(-\omega))^\dagger$, and does not need to be considered explicitly. For this reason, ADC focuses on the forward component, expressing it in the non-diagonal matrix representation:

$$\mathbf{\Pi}^+(\omega) = \mathbf{T}(\omega \mathbf{1} - \mathbf{M})^{-1} \mathbf{T}^\dagger \quad (3)$$

Expanding the effective Hamiltonian (\mathbf{M}) and transition moments (\mathbf{T}) matrices in the Møller–Plesset perturbation series⁹⁷ up to order n

$$\mathbf{M} \approx \mathbf{M}^{(0)} + \mathbf{M}^{(1)} + \dots + \mathbf{M}^{(n)}, \quad (4)$$

$$\mathbf{T} \approx \mathbf{T}^{(0)} + \mathbf{T}^{(1)} + \dots + \mathbf{T}^{(n)} \quad (5)$$

defines the n th-order single-reference ADC method (ADC(n)). An alternative approach that constructs the ADC approximations for the polarization propagator using multireference perturbation theory has been described elsewhere.^{74,98}

ADC allows to directly calculate excitation energies as eigenvalues of the effective Hamiltonian matrix \mathbf{M}

$$\mathbf{M}\mathbf{Y} = \mathbf{Y}\Omega \quad (6)$$

The resulting eigenvectors \mathbf{Y} are used to calculate the ADC(n) spectroscopic amplitudes $\mathbf{X} = \mathbf{T}\mathbf{Y}$, which are combined with transition dipole moment matrix elements ($\mu_{\alpha,pq}$, $\alpha = x, y, z$) to compute oscillator strengths

$$f_m = \frac{2}{3} \Omega_m \sum_{\alpha=x,y,z} \left(\sum_{pq} \mu_{\alpha,pq} X_{pq,m} \right)^2 \quad (7)$$

for the electronic transition with excitation energy Ω_m ($m > 0$).

Matrix elements of \mathbf{M} derived using the effective Liouvillian approach^{74,99–101} for each perturbation order (n) have the form:

$$M_{\mu\nu}^{(n)} = \sum_{klm}^{k+l+m=n} \langle \Phi | [h_\mu^{(k)}, [\tilde{H}^{(l)}, h_\nu^{(m)\dagger}]] | \Phi \rangle \quad (8)$$

where $|\Phi\rangle$ denotes the reference Hartree–Fock wavefunction, $\tilde{H}^{(l)}$ is the l th-order contribution to the effective Hamiltonian (see Ref. 74 for explicit expressions), and $h_\nu^{(m)\dagger}$ are the excitation operators that form the basis of electronic configurations for representing excited states. In the low-order ADC(n) approximations ($n \leq 3$), only two types of $h_\nu^{(m)\dagger}$ need to be considered: the

single-excitation operators $h_\nu^{(0)\dagger} = a_a^\dagger a_i$ and the double-excitation operators $h_\nu^{(1)\dagger} = a_a^\dagger a_b^\dagger a_j a_i$, where i, j and a, b denote occupied and virtual molecular orbitals, respectively. The resulting electronic configurations $h_\nu^{(m)\dagger} |\Phi\rangle$ are schematically depicted in Figure 1. Similarly, the n th-order contributions to the matrix elements of \mathbf{T} can be expressed as:

$$T_{pq\mu}^{(n)} = \sum_{kl}^{k+l=n} \langle \Phi | [\tilde{q}_{pq}^{(k)}, h_\nu^{(l)\dagger}] | \Phi \rangle, \quad (9)$$

where $\tilde{q}_{pq}^{(k)}$ is the k th-order effective observable operator⁷⁴ with $\tilde{q}_{pq}^{(0)} = a_p^\dagger a_q - \langle \Phi | a_p^\dagger a_q | \Phi \rangle$.

The \mathbf{M} and \mathbf{T} matrices have special perturbative structures that are depicted in Figure 2 for the low-order ADC methods. In addition to the strict second-order (ADC(2)) and third-order (ADC(3)) approximations, in this work we will also consider the “extended” second-order method (ADC(2)-X), which improves the description of double excitations by incorporating third-order electron correlation effects.

B. Spin expectation values and contamination in ADC

The single-reference ADC calculations of open-shell molecules may suffer from spin symmetry breaking in (i) the reference Hartree–Fock (HF) wavefunction and/or (ii) the eigenvectors of ADC(n) effective Hamiltonian matrix representing excited states. The reference spin contamination (SC) originates from using the unrestricted HF (UHF) molecular orbitals and can be eliminated by employing the restricted open-shell HF (ROHF) reference instead. The SC in ADC(n) eigenvectors arises when the manifold of excitations described by the operators $h_\nu^{(m)\dagger}$ (Figure 1) is incomplete for representing a particular spin eigenstate. The spin symmetry breaking of this kind cannot be completely eliminated even when using the ROHF reference wavefunction, unless rigorous spin adaptation of equations is performed.

For an approximate wavefunction $|\Psi\rangle$ corresponding to an exact eigenstate with quantum number S , the SC in atomic units is defined as:^{62,102,103}

$$\begin{aligned} \Delta S^2 &= \langle \Psi | \hat{S}^2 | \Psi \rangle - S(S+1) \\ &\equiv \langle S^2 \rangle - S(S+1) \end{aligned} \quad (10)$$

where \hat{S}^2 is the spin-square operator. Calculating ΔS^2 requires evaluating the expectation value $\langle \Psi | \hat{S}^2 | \Psi \rangle$, which can be expressed as^{104–107}

$$\begin{aligned} \langle S^2 \rangle &= \frac{1}{4} \left(\sum_{p \in \alpha} \gamma_p^p - \sum_{\bar{p} \in \beta} \gamma_{\bar{p}}^{\bar{p}} \right)^2 \\ &+ \frac{1}{2} \left(\sum_{p \in \alpha} \gamma_p^p + \sum_{\bar{p} \in \beta} \gamma_{\bar{p}}^{\bar{p}} \right) + \sum_{\substack{p, s \in \alpha \\ \bar{q}, \bar{r} \in \beta}} S_r^p S_s^{\bar{q}} \Gamma_{\bar{r}s}^{p\bar{q}} \end{aligned} \quad (11)$$

in terms of the overlap matrix ($S_q^p = \langle \phi_p | \phi_q \rangle$) and the one- and two-particle reduced density matrices ($\gamma_q^p = \langle \Psi | a_p^\dagger a_q | \Psi \rangle$ and $\Gamma_{rs}^{pq} = \langle \Psi | a_p^\dagger a_q^\dagger a_s a_r | \Psi \rangle$, respectively). In Eq. (11), a bar is used to distinguish the spin-up and spin-down molecular orbitals from each other.

To compute $\langle S^2 \rangle$ and ΔS^2 in ADC calculations of electronic excitations, we derived the equations for γ_q^p and Γ_{rs}^{pq} using the formalism of effective Liouvillian theory.^{74,92,99–101} Defining $K \equiv a_p^\dagger a_q$ or $a_p^\dagger a_q^\dagger a_s a_r$, the density matrices for the I th excited state described by the ADC eigenvector $Y_{\nu I}$ are expressed as:⁹²

$$\langle K \rangle_I = \sum_{(m)} \sum_{\mu\nu} Y_{I\mu}^\dagger K_{\mu\nu}^{(m)} Y_{\nu I} \quad (12)$$

where (n) indicates the perturbation order of ADC(n) approximation and $K_{\mu\nu}^{(m)}$ is the m th-order contribution to the matrix elements of effective density operator (\tilde{K}):

$$K_{\mu\nu}^{(n)} = \sum_{klm}^{k+l+m=n} \langle \Phi | h_\mu^{(k)} \tilde{K}^{(l)} h_\nu^{(m)\dagger} | \Phi \rangle. \quad (13)$$

The operators $\tilde{K}^{(l)}$ at each order l are obtained from the perturbative analysis of Baker–Campbell–Hausdorff expansion of \tilde{K} , as described in Ref. 92. Combining Eqs. (12) and (13) allows to obtain the expressions for γ_q^p and Γ_{rs}^{pq} , which are provided in the Supplementary Material and can be used to evaluate $\langle S^2 \rangle$ and ΔS^2 for any excited state in ADC calculations. We note that an alternative approach for calculating operator expectation values in ADC based on intermediate state representation was developed by Schirmer, Trofimov, Dempwolff, and co-workers.^{72,108–113}

III. IMPLEMENTATION AND COMPUTATIONAL DETAILS

To carry out the calculations of ADC excitation energies, oscillator strengths, and spin contamination, we developed a new ADC implementation in the PySCF package¹¹⁴ that supports the UHF and ROHF reference wavefunctions. The ROHF-based ADC methods incorporated the first-order single excitation amplitudes and off-diagonal elements of Fock matrix in their equations as described in Ref. 92. The calculations of spin expectation values and contamination were performed using the excited-state reduced density matrices discussed in Section II B. To reduce the cost of ADC(3) computations, two approximations were introduced: 1) third-order amplitudes were neglected in the effective transition moments matrix \mathbf{T} and 2) the contributions from $(k, l, m) = (0, 3, 0), (1, 2, 0)$, and $(0, 2, 1)$ in Eq. (13) were omitted in the excited-state one- and two-particle reduced density matrices. No approximations were introduced for ADC(2) and ADC(2)-X. All ADC calculations were per-

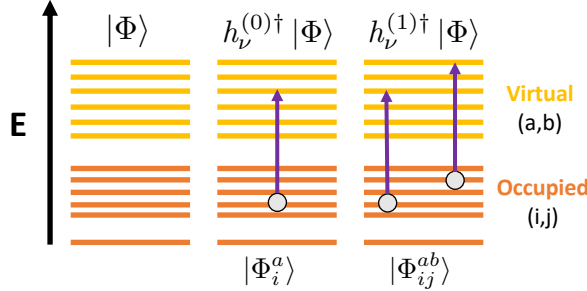


FIG. 1: Electronic configurations $h_\nu^{(m)\dagger} |\Phi\rangle$ ($m = 0, 1$) used for representing the excited states in low-order ADC(n) approximations ($n \leq 3$), relative to the Hartree–Fock reference wavefunction $|\Phi\rangle$.

ADC(2)		ADC(2)-X		ADC(3)	
	$ \Phi_i^a\rangle$	$ \Phi_{ij}^{ab}\rangle$		$ \Phi_i^a\rangle$	$ \Phi_{ij}^{ab}\rangle$
$\langle\Phi_k^c $	2	1		2	1
	1	0		1	1
$\langle\Phi_{kl}^{cd} $	1	0		2	1
	2	1		3	2
\mathbf{T}	\tilde{q}_{pq}	2		2	2
		1		3	2

FIG. 2: Schematic illustration of perturbative structure in the \mathbf{M} and \mathbf{T} matrices. The wavefunctions $|\Phi_i^a\rangle$ and $|\Phi_{ij}^{ab}\rangle$ indicate single and double excitations relative to the Hartree–Fock reference, respectively (Figure 1). Numbers denote the perturbation order at which the expansions of effective Hamiltonian \tilde{H} and observable \tilde{q}_{pq} operators are truncated in each block.

formed using density fitting,^{115–118} correlating all electrons in each molecule.

To assess the effect of spin contamination on the accuracy of ADC(2), ADC(2)-X, and ADC(3) excitation energies (Section IV A), we performed calculations for the benchmark set of open-shell molecules developed by Loos and co-workers.¹¹⁹ The aug-cc-pVQZ (X = D, T) basis sets^{120–123} were employed in this study, with the cc-pVQZ-RI (X = D, T) auxiliary basis sets^{124,125} used to approximate the two-electron integrals in density fitting. The aug-cc-pVDZ results are provided in the Supplementary Material. The molecular geometries were taken from Ref. 119.

To correlate spin contamination with the errors in ADC oscillator strengths in Section IV B, transition properties were computed using linear-response coupled cluster theory with single, double, and triple excitations and ROHF reference (LR-CCSDT/ROHF). These calculations were performed using the aug-cc-pVDZ basis set and the MRCC package.^{126,127}

Finally, in the study of phenyl radical UV/Vis spectrum (Section IV C), the equilibrium geometry was optimized at the MP2 level of theory with the aug-cc-pVTZ

basis set, the UHF reference wavefunction, and the Q-Chem software package.¹²⁸ The ADC(2) and ADC(2)-X simulations of UV/Vis spectra were performed using the aug-cc-pVTZ basis set. Due to the high computational cost, the ADC(3) calculations were performed using the modified aug-cc-pVTZ basis set where the f functions were removed for all carbon atoms. Numerical tests on smaller systems demonstrated the high accuracy of this approximation. The UV/Vis spectra were simulated by plotting a spectral function of the form:

$$T(\omega) = -\frac{1}{\pi} \text{Im} \left[\sum_k \frac{f_k}{\omega - \Omega_k + i\eta} \right] \quad (14)$$

where f_k and Ω_k are the oscillator strength (Eq. (7)) and energy of the k th transition, η is a broadening parameter set to 500 cm^{-1} .

IV. RESULTS AND DISCUSSION

A. Spin contamination and errors in excitation energies

TABLE I: Spin contamination (ΔS^2 , a.u.) in the excited states of weakly spin-contaminated molecules computed using the ADC methods with the UHF or ROHF reference and the aug-cc-pVTZ basis set. The second column reports the spin contamination in the reference UHF wavefunction.

Molecule	Reference	Excitation	ADC(2)	ADC(2)-X	ADC(3) ^a	ADC(2)	ADC(2)-X	ADC(3) ^a	
	UHF		UHF	UHF	UHF	ROHF	ROHF	ROHF	
BeF	0.00	$2\Sigma^+ \rightarrow 2\Pi$	0.00	0.00	0.00	0.00	0.00	0.00	
		$2\Sigma^+ \rightarrow 2\Sigma^+$	0.01	0.01	0.01	0.00	0.01	0.00	
BeH	0.00	$2\Sigma^+ \rightarrow 2\Pi$	0.01	0.02	0.02	0.01	0.02	0.02	
		$2\Sigma^+ \rightarrow 2\Pi$	0.03	0.03	0.02	0.01	0.03	0.02	
BH ₂	0.00	$2A_1 \rightarrow 2B_1$	0.02	0.03	0.03	0.02	0.03	0.02	
		$2B_2 \rightarrow 2B_1$	0.03	0.04	0.04	0.03	0.03	0.03	
OH	0.01	$2\Sigma^+ \rightarrow 2\Sigma^+$	0.03	0.04	0.04	0.03	0.03	0.03	
		$2B_2 \rightarrow 2A_1$	0.04	0.04	0.04	0.03	0.03	0.03	
F ₂ BO	0.01	$2B_1 \rightarrow 2A_1$	0.04	0.04	0.04	0.03	0.03	0.03	
		$2B_2 \rightarrow 2A_1$	0.03	0.04	0.04	0.03	0.03	0.03	
NH ₂	0.01	$2A_1 \rightarrow 2A_1$	0.04	0.05	0.04	0.03	0.03	0.03	
		$2A_2' \rightarrow 2A_1'$	0.02	0.02	0.02	0.01	0.01	0.01	
CH ₃	0.01	$2A_2' \rightarrow 2E'$	0.03	0.06	0.05	0.02	0.04	0.04	
		$2A_2' \rightarrow 2E'$	0.03	0.03	0.03	0.02	0.01	0.01	
HOC	0.01	$2A_2' \rightarrow 2A''$	0.02	0.03	0.03	0.01	0.01	0.01	
		$2A_1' \rightarrow 2A''$	0.04	0.05	0.04	0.03	0.03	0.02	
F ₂ BS	0.01	$2B_2 \rightarrow 2B_1$	0.05	0.06	0.06	0.03	0.04	0.04	
		$2B_2 \rightarrow 2A_1$	0.05	0.06	0.06	0.04	0.05	0.04	
HCO	0.02	$2A' \rightarrow 2A''$	0.08	0.09	0.06	0.09	0.09	0.05	
		$2A' \rightarrow 2A'$	0.13	0.12	0.10	0.14	0.12	0.08	
H ₂ BO	0.02	$2B_2 \rightarrow 2B_1$	0.04	0.05	0.04	0.03	0.03	0.03	
		$2B_2 \rightarrow 2A_1$	0.05	0.06	0.05	0.03	0.04	0.03	
PH ₂	0.02	$2B_1 \rightarrow 2A_1$	0.04	0.06	0.05	0.03	0.04	0.04	
		$2A' \rightarrow 2A''$	0.09	0.11	0.11	0.07	0.08	0.09	
H ₂ PO	0.04	$2A' \rightarrow 2A''$	0.05	0.07	0.07	0.07	0.09	0.10	
		$2A' \rightarrow 2A'$	0.08	0.10	0.09	0.04	0.05	0.05	
H ₂ PS	0.04	$2A' \rightarrow 2A''$	0.08	0.10	0.09	0.06	0.08	0.07	
		$2A' \rightarrow 2A'$	0.06	0.08	0.08	0.06	0.08	0.07	
NO	0.04	$2\Pi \rightarrow 2\Sigma^+$	0.13	0.13	0.09	0.09	0.09	0.06	
		$2\Pi \rightarrow 2\Sigma^+$	0.13	0.12	0.08	0.09	0.08	0.05	
Sum			1.34	1.55	1.32	1.05	1.21	1.01	
Average			0.05	0.06	0.05	0.04	0.04	0.04	
Minimum			0.00	0.00	0.00	0.00	0.00	0.00	
Maximum			0.13	0.13	0.11	0.14	0.12	0.10	

^a ADC(3) ΔS^2 was computed using the ADC(2)-X density matrices and ADC(3) eigenvectors of effective Hamiltonian matrix (Section III).

TABLE II: Spin contamination (ΔS^2 , a.u.) in the excited states of strongly spin-contaminated molecules computed using the ADC methods with the UHF or ROHF reference and the aug-cc-pVTZ basis set. The second column reports the spin contamination in the reference UHF wavefunction.

Molecule	Reference	Excitation	ADC(2)	ADC(2)-X	ADC(3) ^a	ADC(2)	ADC(2)-X	ADC(3) ^a	
	UHF		UHF	UHF	UHF	ROHF	ROHF	ROHF	
CNO	0.06	$2\Pi \rightarrow 2\Sigma^+$	0.25	0.21	0.29	0.29	0.24	0.33	
		$2\Pi \rightarrow 2\Pi$	0.12	0.12	0.24	0.14	0.35	0.13	
NCO	0.09	$2\Pi \rightarrow 2\Sigma^+$	0.60	0.30	0.62	0.47	0.49	0.41	
		$2\Pi \rightarrow 2\Pi$	0.13	0.15	0.14	0.05	0.06	0.05	
Vinyl	0.20	$2A' \rightarrow 2A''$	0.07	0.06	0.07	0.05	0.05	0.05	
		$2A' \rightarrow 2A''$	0.11	0.11	0.11	0.07	0.08	0.07	
Allyl	0.20	$2A' \rightarrow 2A'$	0.24	0.26	0.25	0.08	0.10	0.09	
		$2A' \rightarrow 2A'$	0.25	0.26	0.26	0.09	0.10	0.10	
CO ⁺	0.22	$2\Sigma^+ \rightarrow 2\Pi$	0.13	0.15	0.15	0.04	0.05	0.07	
		$2\Sigma^+ \rightarrow 2\Sigma^+$	0.28	0.27	0.40	0.06	0.08	0.52	
CH	0.35	$2\Pi \rightarrow 2\Delta$	0.08	0.48	0.04	0.02	0.01	0.01	
		$2\Pi \rightarrow 2\Delta$	0.04	0.05	0.67	0.02	0.30	0.10	
CN	0.40	$2\Sigma^+ \rightarrow 2\Pi$	0.20	0.21	0.22	0.04	0.05	0.06	
		$2\Sigma^+ \rightarrow 2\Sigma^+$	0.39	0.37	0.40	0.05	0.07	0.15	
Nitromethyl	0.42	$2B_1 \rightarrow 2B_2$	0.61	0.51	0.65	0.30	0.30	0.49	
		$2B_1 \rightarrow 2A_2$	0.29	0.21	0.27	0.61	0.45	0.65	
CON	0.68	$2B_1 \rightarrow 2A_1$	0.54	0.58	0.53	0.26	0.27	0.40	
		$2B_1 \rightarrow 2B_1$	0.30	0.21	0.43	0.13	0.17	0.16	
Sum			6.61	6.50	7.99	3.51	4.26	5.26	
Average			0.28	0.27	0.33	0.15	0.18	0.22	
Minimum			0.04	0.05	0.04	0.02	0.01	0.01	
Maximum			0.78	0.88	0.92	0.61	0.56	0.68	

^a ADC(3) ΔS^2 was computed using the ADC(2)-X density matrices and ADC(3) eigenvectors of effective Hamiltonian matrix (Section III).

We begin by investigating the effect of ground- and excited-state spin contamination (ΔS^2) on the accuracy of ADC excitation energies. We conduct our study for the benchmark set of Loos and co-workers,¹¹⁹ which contains highly accurate reference excitation energies for 24 open-shell molecules. To organize our discussion, we split the molecules in this set into two groups: i) weakly spin-contaminated (WSM) with the UHF $\Delta S^2 \leq 0.05$ (15 molecules) and ii) strongly spin-contaminated (SSM) with the UHF $\Delta S^2 > 0.05$ (9 molecules).

Tables I and II show the excited-state ΔS^2 for WSM and SSM, respectively, computed using ADC(2), ADC(2)-X, and ADC(3) starting with either the UHF or ROHF reference wavefunction. As the ground-state UHF ΔS^2 increases, the ADC methods tend to exhibit higher spin contamination in the excited states. This can be observed in the total, average, and maximum ΔS^2 that are significantly higher for SSM compared to WSM. While for WSM ΔS^2 is relatively insensitive to the choice of reference wavefunction, using the ROHF reference in ADC calculations helps to significantly reduce ΔS^2 for SSM.

Contrary to what might be expected, ADC(3) tends to show higher spin contamination in its excited states than ADC(2) and ADC(2)-X, which suggests that increasing the level of theory may worsen the description of electronic spin in the unrestricted ADC calculations for SSM. This is particularly noticeable for the ROHF-based ADC methods where the total and average ΔS^2 of SSM increases by $\sim 47\%$ from ADC(2) to ADC(3). We note that this trend may be affected by the approximations in ADC(3) calculations of ΔS^2 , which employed the ADC(2)-X reduced density matrices and ADC(3) eigenvectors of effective Hamiltonian matrix (Section III). However, an increase in ΔS^2 from ADC(2) to ADC(3) was also observed in the ADC calculations of charged excitations where no approximations in the ADC(3) density matrices were introduced.⁹²

To analyze the effect of ΔS^2 on the accuracy of ADC methods, we computed the errors in ADC(2), ADC(2)-X, and ADC(3) excitation energies relative to the accurate reference data from Loos et al.¹¹⁹ These results, along with their statistical analysis, are shown in Tables III and IV for WSM and SSM, respectively. In addition, in Figure 3 the absolute errors in excitation energies are plotted against ΔS^2 for the excited states of SSM. For WSM, the ADC(2) and ADC(3) methods show accurate results with either the UHF or ROHF reference wavefunctions. This is reflected by their mean absolute errors (MAE) and standard deviation of errors (STDV) that do not exceed 0.13 eV. The ADC(2)-X method exhibits much larger MAE (~ 0.5 eV) due to its well-known unbalanced description of electron correlation effects.⁷³

All methods show much higher errors in excitation energies for SSM. This is particularly noticeable for ADC(2), which MAE and STDV grow ~ 4 -fold for both the UHF and ROHF references. The ADC(3) method shows a more modest increase in MAE from WSM to SSM by a factor of ~ 3.5 or ~ 2.5 for when using

the UHF or ROHF orbitals, respectively. Overall, the MAE in excitation energies of SSM reduce in the order ADC(2)/UHF > ADC(3)/UHF > ADC(2)/ROHF > ADC(3)/ROHF, which may be expected due to the higher-order description of electron correlation effects in ADC(3) and lower excited-state ΔS^2 in the calculations with ROHF reference.

A more detailed picture showing the role of spin contamination in ADC calculations of electronic excitations can be obtained by analyzing the data in Figure 3, which plots the absolute errors in excitation energies ($\Delta\Omega_m$) against ΔS^2 for the excited states of SSM. A linear regression analysis of this data reveals that, when using the UHF reference, the ADC methods exhibit correlations between $\Delta\Omega_m$ and ΔS^2 with $R^2 \geq 0.11$. The strongest correlation $R^2 = 0.17$ is observed for ADC(3)/UHF, suggesting that at this level of theory ΔS^2 plays a significant role in determining the errors in excitation energies, together with the approximations in description of electron correlation. The ADC(2) method shows a weaker correlation with $R^2 = 0.11$, which indicates the increased role of approximate electron correlation treatment in determining $\Delta\Omega_m$.

For ADC(2)/UHF, the $\Delta\Omega_m - \Delta S^2$ correlation is negative, leading to smaller errors for the excited states with larger ΔS^2 , as a result of error cancellation. Similar trend has been observed in the ADC(2)/UHF calculations of charged excitation energies, which errors also benefit from error cancellation.⁹² As discussed in Section IVB, this reduction in excitation energy errors at the ADC(2)/UHF level of theory comes at a price of significantly less accurate oscillator strengths. The ADC methods with ROHF reference show little to no correlation between $\Delta\Omega_m$ and ΔS^2 in the linear regression analysis ($R^2 \approx 0.00, 0.04, 0.01$ for ADC(2), ADC(2)-X, ADC(3), respectively), suggesting that the errors of ADC methods with this reference primarily originate from approximations in the description of electron correlation.

B. Spin contamination and errors in oscillator strengths

In addition to excitation energies, reliable simulations of UV/Vis spectra require accurate calculations of transition dipole moments and oscillator strengths. Recently, several benchmark studies of oscillator strengths have been reported for a variety of excited-state electronic structure methods^{129–132} including ADC.^{77,81,88,133,134} All of these studies, however, focused on excited electronic states of closed-shell molecules, which can be simulated with little to no spin contamination by starting with a restricted reference wavefunction.

Here, we assess the accuracy of ADC oscillator strengths (f_m) for open-shell molecules with strong spin contamination in excited states. To quantify the errors in f_m (Δf_m), we computed accurate oscillator strengths using the ROHF-based linear-response coupled cluster theory with up to triple excitations (LR-CCSDT/ROHF)

TABLE III: Vertical excitation energies (eV) of weakly spin-contaminated molecules computed using the ADC methods with the UHF or ROHF reference and the aug-cc-pVTZ basis set. For each method, we report the mean absolute errors (MAE) and standard deviations of errors (STDV) relative to the full configuration interaction (FCI) results from Ref. 119. Minimum (MIN) and maximum (MAX) errors are also shown.

Molecule	Excitation	ADC(2) UHF	ADC(2)-X UHF	ADC(3) UHF	ADC(2) ROHF	ADC(2)-X ROHF	ADC(3) ROHF	FCI
BeF	$^2\Sigma^+ \rightarrow ^2\Pi$	4.21	4.12	4.11	4.20	4.11	4.11	4.14
	$^2\Sigma^+ \rightarrow ^2\Sigma^+$	6.36	6.24	6.23	6.35	6.24	6.23	6.21
BeH	$^2\Sigma^+ \rightarrow ^2\Pi$	2.60	2.35	2.44	2.57	2.33	2.44	2.49
	$^2\Sigma^+ \rightarrow ^2\Pi$	6.54	6.34	6.43	6.53	6.34	6.43	6.46
BH ₂	$^2A_1 \rightarrow ^2B_1$	1.31	0.88	1.11	1.29	0.86	1.11	1.18
	$^2\Sigma^+ \rightarrow ^2\Sigma^+$	4.28	3.66	4.04	4.22	3.62	4.02	4.10
F ₂ BO	$^2B_2 \rightarrow ^2B_1$	0.82	0.30	0.59	0.79	0.27	0.58	0.71
	$^2B_2 \rightarrow ^2A_1$	2.92	2.32	2.73	2.88	2.29	2.72	2.78
NH ₂	$^2B_1 \rightarrow ^2A_1$	2.22	1.65	2.04	2.18	1.61	2.02	2.12
	$^2A''_1 \rightarrow ^2A'_1$	6.02	5.49	5.83	5.96	5.44	5.81	5.85
CH ₃	$^2A''_2 \rightarrow ^2E'$	7.19	6.49	6.92	7.12	6.43	6.89	6.96
	$^2A''_2 \rightarrow ^2E'$	7.34	6.80	7.17	7.27	6.76	7.15	7.18
HOC	$^2A'_1 \rightarrow ^2A''$	7.76	7.29	7.62	7.71	7.26	7.60	7.65
	$^2A' \rightarrow ^2A''$	1.03	0.37	0.71	0.97	0.32	0.69	0.92
F ₂ BS	$^2B_2 \rightarrow ^2B_1$	0.63	-0.03	0.35	0.57	-0.07	0.32	0.48
	$^2B_2 \rightarrow ^2A_1$	3.19	2.39	2.88	3.11	2.33	2.84	2.93
HCO	$^2A' \rightarrow ^2A''$	2.24	1.42	1.92	2.19	1.41	1.92	2.09
	$^2A' \rightarrow ^2A'$	5.38	4.85	5.53	5.38	4.86	5.51	5.42
H ₂ BO	$^2B_2 \rightarrow ^2B_1$	2.10	1.58	1.81	2.01	1.49	1.76	2.15
	$^2B_2 \rightarrow ^2A_1$	3.53	2.88	3.28	3.45	2.80	3.23	3.49
PH ₂	$^2B_1 \rightarrow ^2A_1$	2.98	2.22	2.65	2.88	2.17	2.62	2.77
	$^2A' \rightarrow ^2A''$	3.02	2.26	2.75	2.82	2.03	2.83	2.80
H ₂ PO	$^2A' \rightarrow ^2A'$	4.42	3.73	3.93	4.19	3.42	3.96	4.19
	$^2A' \rightarrow ^2A''$	1.29	0.57	0.97	1.17	0.47	0.89	1.16
H ₂ PS	$^2A' \rightarrow ^2A'$	2.86	2.05	2.49	2.75	1.88	2.39	2.72
	$^2A' \rightarrow ^2\Sigma^+$	6.17	5.50	6.22	6.18	5.52	6.11	6.13
NO	$^2\Pi \rightarrow ^2\Sigma^+$	7.21	6.65	7.34	7.23	6.64	7.35	7.29 ^a
	$^2\Pi \rightarrow ^2\Sigma^+$	7.21	6.65	7.34	7.23	6.64	7.35	7.29 ^a
MAE		0.13	0.45	0.10	0.08	0.50	0.12	
STDV		0.08	0.19	0.11	0.07	0.22	0.12	
MIN		0.04	0.02	0.01	0.00	0.03	0.02	
MAX		0.26	0.67	0.34	0.18	0.84	0.39	

^a Computed using equation-of-motion coupled cluster theory with up to quadruple excitations (EOM-CCSDTQ)¹¹⁹

TABLE IV: Vertical excitation energies (eV) of strongly spin-contaminated molecules computed using the ADC methods with the UHF or ROHF reference and the aug-cc-pVTZ basis set. For each method, we report the mean absolute errors (MAE) and standard deviations of errors (STDV) relative to the full configuration interaction (FCI) results from Ref. 119. Minimum (MIN) and maximum (MAX) errors are also shown.

Molecule	Excitation	ADC(2) UHF	ADC(2)-X UHF	ADC(3) UHF	ADC(2) ROHF	ADC(2)-X ROHF	ADC(3) ROHF	FCI
CNO	$^2\Pi \rightarrow ^2\Sigma^+$	2.45	0.64	1.95	2.47	0.45	1.75	1.61
	$^2\Pi \rightarrow ^2\Pi$	5.70	4.46	5.29	5.58	4.06	5.02	5.57 ^a
NCO	$^2\Pi \rightarrow ^2\Pi$	5.99	4.54	5.59	5.83	4.39	5.17	5.57 ^a
	$^2\Pi \rightarrow ^2\Sigma^+$	3.03	2.18	2.97	2.76	2.00	2.73	2.83
Vinyl	$^2\Pi \rightarrow ^2\Pi$	5.22	3.86	4.64	4.84	3.34	4.60	4.70
	$^2A' \rightarrow ^2A''$	4.05	2.53	3.15	3.54	2.62	3.04	3.26
Allyl	$^2A' \rightarrow ^2A''$	5.20	4.01	4.66	4.93	4.05	4.59	4.69
	$^2A' \rightarrow ^2A'$	6.64	5.81	6.39	6.45	5.59	6.23	5.60
CO ⁺	$^2A' \rightarrow ^2A'$	7.23	6.39	6.98	7.03	6.18	6.82	6.21 ^a
	$^2A_2 \rightarrow ^2B_1$	4.34	2.64	3.38	3.77	2.61	3.12	3.43 ^a
CH	$^2A_2 \rightarrow ^2A_1$	5.34	4.59	5.05	5.01	4.31	4.79	4.97 ^a
	$^2\Pi \rightarrow ^2\Delta$	3.17	2.14	2.33	3.16	1.93	2.06	2.91
CN	$^2\Sigma^+ \rightarrow ^2\Pi$	3.74	1.98	3.78	3.16	2.06	3.56	3.28
	$^2\Sigma^+ \rightarrow ^2\Sigma^+$	5.83	4.38	6.84	4.80	3.98	6.98	5.81
Nitromethyl	$^2B_1 \rightarrow ^2B_2$	2.23	0.91	2.03	2.01	0.92	2.33	2.05 ^a
	$^2B_1 \rightarrow ^2A_2$	2.60	0.58	2.01	2.83	1.19	1.96	2.38 ^a
CON	$^2B_1 \rightarrow ^2A_1$	2.82	1.72	2.98	2.56	1.47	2.70	2.56 ^a
	$^2B_1 \rightarrow ^2B_1$	6.06	4.45	5.21	5.78	4.50	5.19	5.35 ^a
MAE		0.52	0.94	0.38	0.35	0.99	0.32	
STDV		0.40	0.49	0.52	0.43	0.48	0.43	
MIN		0.02	0.18	0.02	0.00	0.01	0.01	
MAX		1.04	1.80	1.30	1.01	1.84	1.17	

^a Computed using equation-of-motion coupled cluster theory with up to triple excitations (EOM-CCSDT)¹¹⁹

and the aug-cc-pVDZ basis set. Due to the challenges associated with performing LR-CCSDT/ROHF calcula-

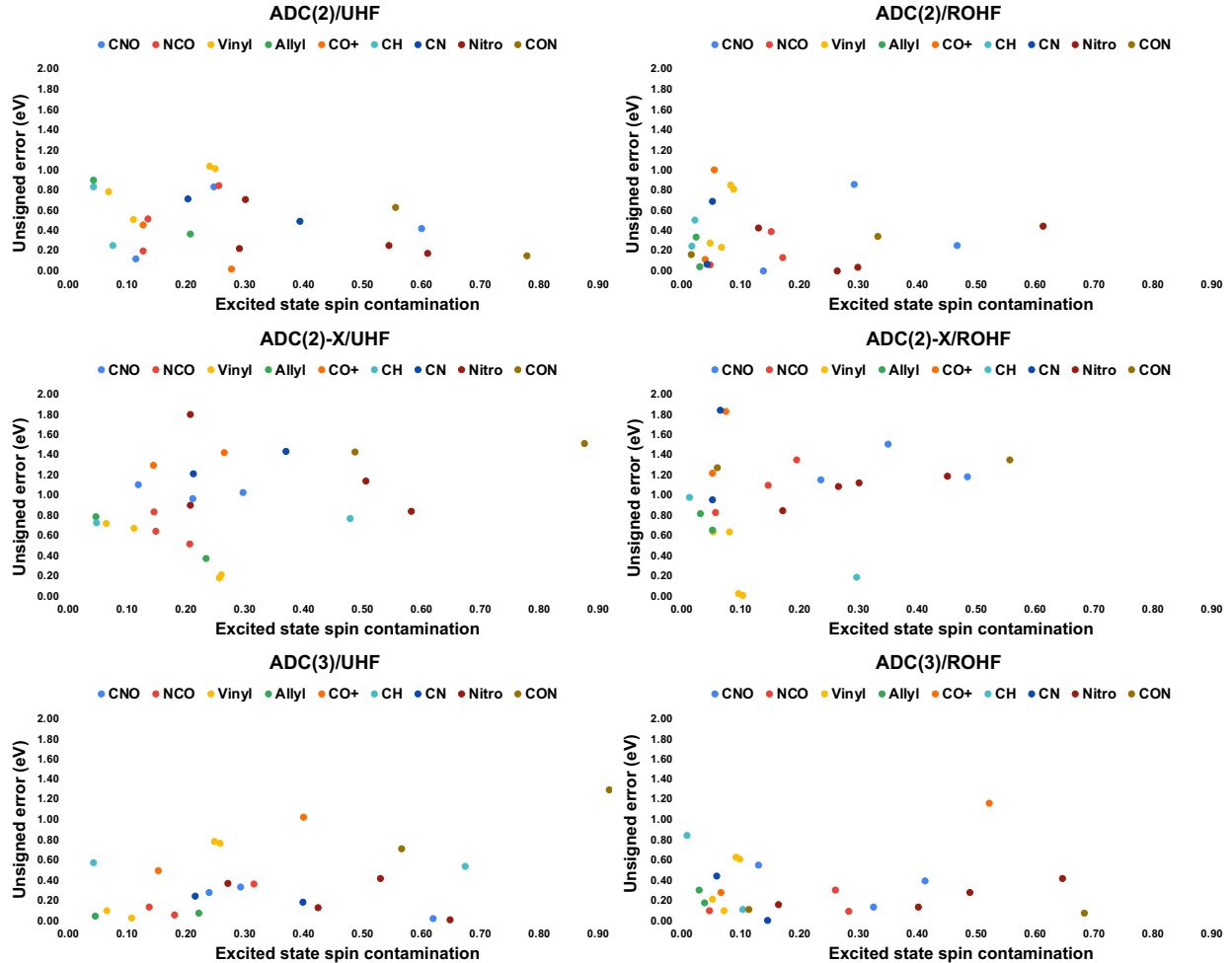


FIG. 3: Unsigned errors in the excitation energies of strongly spin-contaminated molecules plotted against the excited-state spin contamination computed using the ADC methods with the UHF or ROHF reference wavefunctions. See Table IV for details.

tions, only 6 out of 9 SSM from Section IV A were included in this study. The ADC and LR-CCSDT/ROHF oscillator strengths are reported in the Supplementary Material.

Figure 4 plots Δf_m against ΔS^2 for each electronic transition. The UHF-based ADC methods exhibit positive correlations between Δf_m and ΔS^2 in the linear regression analysis, suggesting that the excited states with larger ΔS^2 are more likely to show large errors in Δf_m than those with smaller ΔS^2 . The strongest correlations are observed for ADC(2) ($R^2 = 0.12$) and ADC(3) ($R^2 = 0.10$), while for ADC(2)-X this trend is less pronounced ($R^2 = 0.04$). Using the ROHF reference lowers the average and maximum error in f_m for all ADC methods. In addition, the ROHF-based ADC methods show significantly weaker $\Delta f_m - \Delta S^2$ correlations with R^2 ranging from 0.00 to 0.06. Overall, these results highlight that the correct description of electronic spin is important for accurate calculations of oscillator strengths and provide evidence that the transition properties calculated using the ADC methods can be susceptible to

spin contamination, particularly at low perturbation orders.

C. Case study: spin contamination in the UV/Vis spectrum of phenyl radical

Having analyzed the effect of spin contamination on the ADC excitation energies and oscillator strengths, we now take a closer look at how this unphysical spin symmetry breaking manifests itself in the ADC simulations of UV/Vis spectra. For this study, we focus on phenyl radical (C_6H_5), which plays an important role in organic synthesis, environmental chemistry, combustion reactions, and chemical processes in interstellar objects.^{135–142} Despite being the smallest aromatic radical,¹⁴³ C_6H_5 has a nontrivial electronic structure in its \tilde{X}^2A_1 ground state with a heavily spin-contaminated UHF wavefunction ($\Delta S^2 = 0.40$ a.u. at the MP2/aug-cc-pVTZ optimized geometry), which presents challenges for simulating its UV/Vis spectrum using single-reference electronic

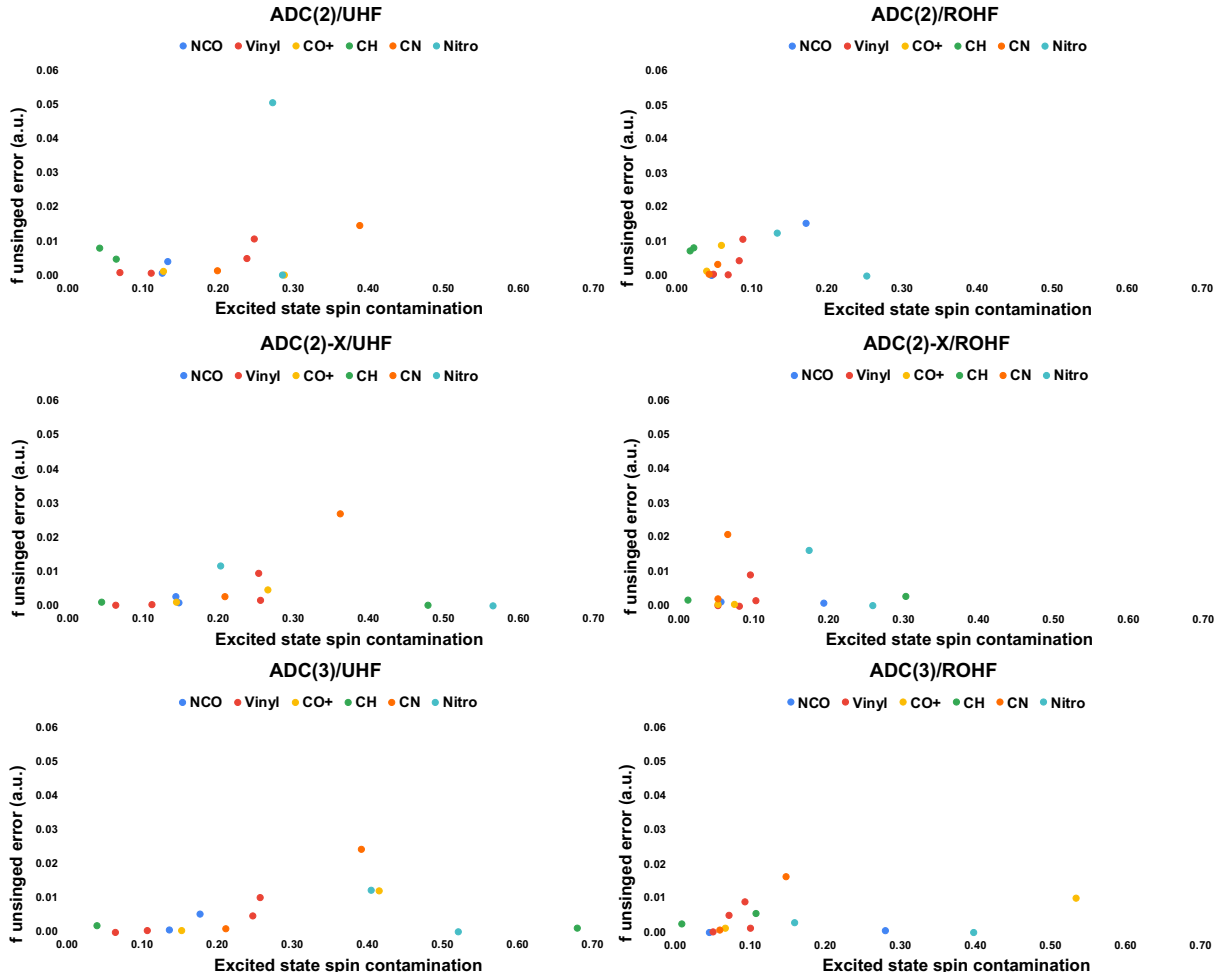


FIG. 4: Unsigned errors in the oscillator strengths of strongly spin-contaminated molecules plotted against the excited-state spin contamination computed using the ADC methods with the UHF or ROHF reference wavefunctions. Calculations were performed using the aug-cc-pVDZ basis. See Section III and Supplementary Materials for details.

structure methods.¹⁴⁴

Several experimental studies of phenyl radical UV/Vis absorption have been reported.^{145–152} The most complete UV/Vis spectrum of C₆H₅ in the 52632 – 4000 cm⁻¹ range was measured in a noble gas matrix by Radziszewski¹⁵³ and is shown in Figure 5. In this spectrum, three regions can be identified: 1) a very weak broad feature between 25000 and 17500 cm⁻¹ centered at \sim 21500 cm⁻¹ (shaded orange), 2) a broad (45000 – 40000 cm⁻¹) band with medium intensity and a maximum at \sim 43000 cm⁻¹ (shaded blue), and 3) a higher-energy region (> 46000 cm⁻¹) with three intense peaks at 47365, 48430, and 49838 cm⁻¹ (shown as dashed lines).

Extensive theoretical studies of C₆H₅ UV/Vis spectra and excited states have been also performed.^{75,150,154–158} While all reported calculations were in agreement with the experiments about the nature of electronic transition in region 1, some of them provided different interpretations of spectral features in region 2 and 3.^{75,157} In addition, the simulated UV/Vis spectra revealed strong

dependence on the level of theory used in calculations.

Here, we investigate the phenyl radical UV/Vis spectrum using the ADC methods and the large aug-cc-pVTZ basis set, paying particular attention to the spin contamination in its excited states. To organize our discussion, we focus on each of three regions in Figure 5 one at a time, starting with the lowest-energy electronic transition.

1. Region 1 (25000 – 17500 cm⁻¹)

This region of experimental UV/Vis spectrum (Figure 5) consists of a broad band with low intensity centered at \sim 21500 cm⁻¹.¹⁵³ Previous experimental and theoretical studies assigned this spectral feature as excitation from the ground \tilde{X}^2A_1 state to an excited state of 2B_1 symmetry.^{75,145,151,154–158} In agreement with this assignment, the ADC-simulated UV/Vis spectra (Figure 5) show a low-energy transition to the 2B_1 state

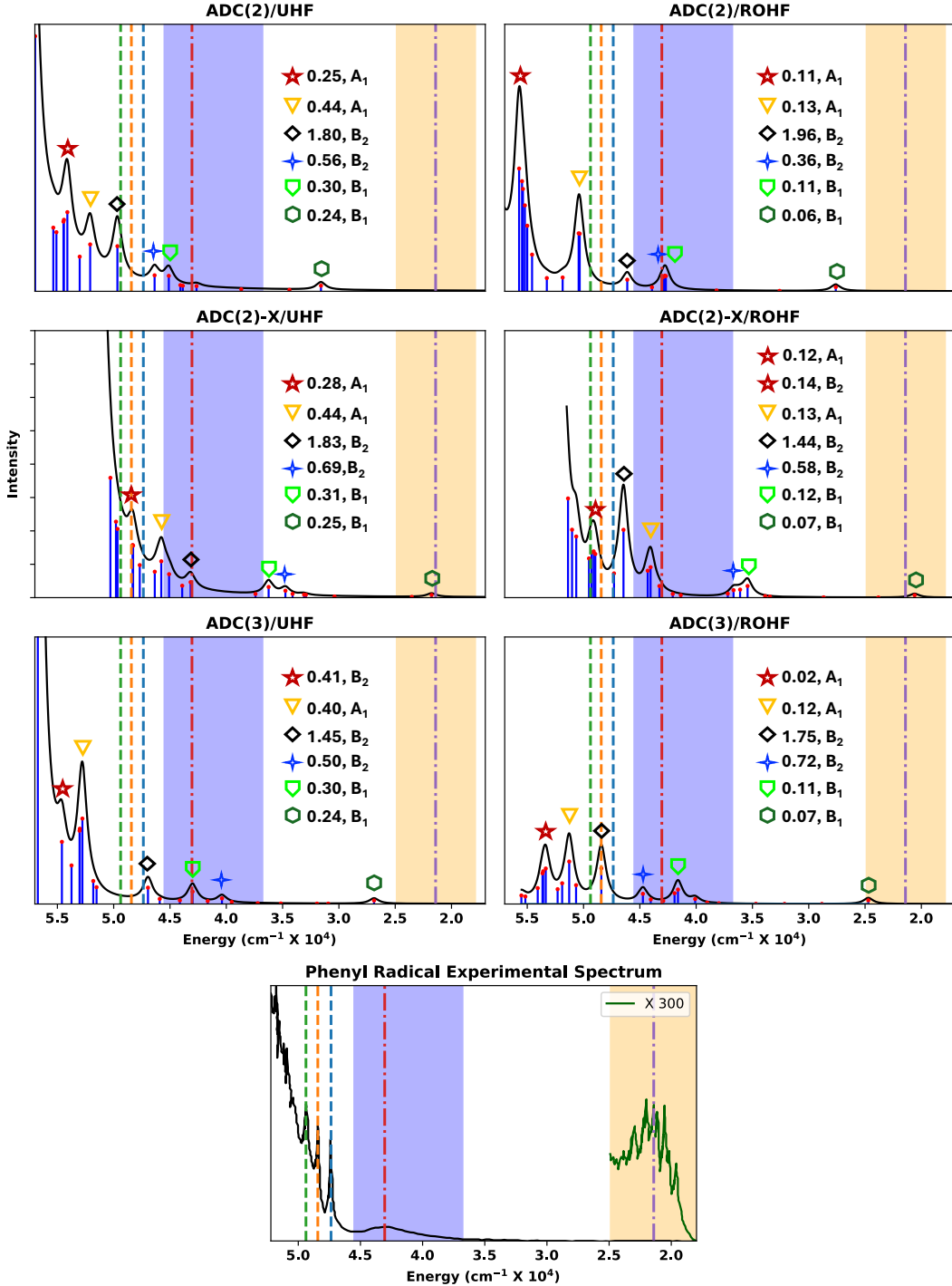


FIG. 5: The UV/Vis spectra of phenyl radical measured experimentally¹⁵³ and simulated using the gvADC methods. Prominent features in the experimental spectrum are highlighted with shading or dashed vertical lines. For the peaks labeled in simulated spectra, the spin contamination and spatial symmetry of corresponding excited states are provided in the legend. See Section III and Supplementary Materials for computational details and complete data.

with a small oscillator strength. When combined with the UHF reference, the ADC(2) method strongly overestimates the excitation energy for this state, predicting it to be $\sim 6500 \text{ cm}^{-1}$ outside the experimental range. The ADC(2)-X/UHF and ADC(3)/UHF methods show

better agreement with the experiment. All UHF-based ADC calculations exhibit significant spin contamination in the 2B_1 excited state with $\Delta S^2 \sim 0.25 \text{ a.u.}$

Using the ROHF reference reduces the 2B_1 spin contamination by a factor of three and lowers its excita-

tion energy by $\sim 4000 \text{ cm}^{-1}$ for ADC(2), $\sim 1200 \text{ cm}^{-1}$ for ADC(2)-X, and $\sim 2000 \text{ cm}^{-1}$ for ADC(3), significantly improving their agreement with the experimental results. Reducing spin contamination lowers the oscillator strength computed using ADC(2), but has a minor effect on transition intensities obtained from ADC(2)-X and ADC(3). Although the ADC(2)-X/ROHF excitation energy appears to be in a better agreement with the experiment than ADC(3)/ROHF, we note that the simulated spectra reflect vertical excitation energies and that including excited-state structural relaxation and vibrational effects is expected to improve the performance of ADC(3)/ROHF relative to ADC(2)-X/ROHF.

2. Region 2 ($45000 - 40000 \text{ cm}^{-1}$)

In this region, the experimental UV/Vis spectrum (Figure 5) exhibits a broad signal with medium intensity and a maximum at $\sim 43000 \text{ cm}^{-1}$.¹⁵³ Although this feature was experimentally assigned as an excitation to the 2A_1 state, theoretical studies suggested that the absorption in this region is dominated by the electronic excitations to either 2B_1 or 2B_2 , with some disagreement between different levels of theory.^{75,157} Indeed, the ADC-simulated UV/Vis spectra reported in Figure 5 exhibit several peaks near the $45000 - 40000 \text{ cm}^{-1}$ region with the most intense transitions identified as excitations to the 2B_1 or 2B_2 states. The relative energies, intensities, and order of these states, however, strongly depend on the level of theory and reference wavefunction.

The ADC(2)/UHF method predicts very similar intensities for the 2B_1 and 2B_2 transitions and overestimates their energies relative to the experimental results. Increasing the level of electron correlation treatment to ADC(3)/UHF lowers the 2B_1 and 2B_2 excitation energies, changes their order in the energy spectrum, and decreases the intensity of 2B_2 relative to 2B_1 . Both 2B_1 and 2B_2 exhibit strong spin contamination with $\Delta S^2 \sim 0.30$ and 0.55 a.u., respectively.

Combining ADC(2) with the ROHF reference decreases ΔS^2 in both 2B_1 and 2B_2 , lowers their excitation energy by up to $\sim 3000 \text{ cm}^{-1}$, and improves the agreement of simulations with experiment. For ADC(3), reducing spin symmetry breaking in the reference wavefunction changes the peak structure in the $45000 - 40000 \text{ cm}^{-1}$ region where a new 2B_2 peak appears at higher energy ($\sim 45000 \text{ cm}^{-1}$), with intensity somewhat lower than that of 2B_1 and large $\Delta S^2 = 0.72$ a.u. Among all ADC methods employed in this work, ADC(3)/ROHF shows the best agreement with experiment in this region, despite exhibiting strong spin contamination in its results.

3. Region 3 ($> 46000 \text{ cm}^{-1}$)

Finally, we consider the highest energy region ($> 46000 \text{ cm}^{-1}$) where the experimental UV/Vis spectrum shows three peaks with high intensity at ~ 47360 , 48430, and 49840 cm^{-1} , labeled with dashed lines in Figure 5.¹⁵³ The lowest-energy peak in this region (47360 cm^{-1}) has been experimentally assigned as a transition to the 2B_2 excited state,¹⁵³ but the theoretical studies using MRCI and ADC(2)-X/UHF with smaller basis sets than the one employed in this work labeled this excitation as 2B_1 .^{75,157} No reliable assignments have been made for the two higher-energy features at 48430 and 49840 cm^{-1} .

The ADC-simulated UV/Vis spectra consistently show three intense peaks with transition energies $\gtrsim 45000 \text{ cm}^{-1}$, but the relative spacing, order, and intensities of the corresponding excited states vary significantly depending on the level of theory and reference wavefunction employed. With the exception of ADC(2)/ROHF, all ADC calculations assign the lowest-energy peak in this region as a transition to the 2B_2 state, which agrees with the experimental interpretation¹⁵³ but contradicts prior theoretical assignments.^{75,157} Same methods also assign the second-energy feature as excitation to the 2A_1 state. The assignment of the highest-energy peak is complicated due to the high density of states, but most methods reveal strong absorption from the higher-lying 2A_1 with a significant contribution from 2B_2 .

When using the UHF reference, all excited states in this region show strong spin contamination. The highest degree of spin symmetry breaking is observed for the lowest-energy 2B_2 state where ΔS^2 ranges from 1.45 to 1.83 a.u. depending on the level of theory used. Starting the calculations with the ROHF reference has a profound effect on the simulated UV/Vis spectra, changing the order of peaks, their spacing, and relative intensities. Although reducing spin contamination in the reference wavefunction helps to lower ΔS^2 for the 2A_1 excited states, the lowest-energy 2B_2 state remains highly spin-contaminated. Neither method produces UV/Vis spectra in satisfactory agreement with the experiment, although increasing the basis set size and incorporating effects of excited-state structural relaxation may improve the results. Nevertheless, the residual spin contamination in the calculated UV/Vis spectra is concerning and warrants the development of spin-adapted ADC methods for open-shell systems.

V. CONCLUSIONS

In this work, we performed a systematic study of spin contamination (SC) in the calculations of excited electronic states and UV/Vis spectra of open-shell molecules using algebraic diagrammatic construction theory (ADC). As a perturbation theory, ADC offers a hierarchy of excited-state methods that can deliver accurate results more efficiently than the non-perturbative

approaches such as coupled cluster theory. These computational savings come at a cost of higher sensitivity to the quality of reference wavefunction, which can be especially problematic for open-shell systems.

Our work reports several important findings about the role of SC in the ADC calculations of excitation energies, oscillator strengths, and UV/Vis spectra. First, we demonstrate that the accuracy of ADC methods strongly depends on the level of SC in the UHF reference wavefunction. In particular, for open-shell molecules with the UHF SC ≤ 0.05 a.u., the second-order (ADC(2)) and third-order (ADC(3)) ADC methods exhibit high accuracy with the errors of ~ 0.1 eV in excitation energy, on average. However, when applied to strongly spin-contaminated molecules with the UHF SC > 0.05 a.u., their performance significantly deteriorates. One of the factors contributing to this poorer performance is the SC in excited states, which increases significantly as the reference SC grows. Performing the ADC calculations with the ROHF reference wavefunctions allows to significantly reduce the level of SC in the excited states, but does not eliminate it entirely. Increasing the level of theory from ADC(2) to ADC(3) does not help reducing the spin symmetry breaking in excited states, and may lead to increasing SC instead.

Our second finding is that SC can significantly affect the accuracy of ADC oscillator strengths and calculated UV/Vis spectra. In particular, we demonstrated that the molecules with strong SC in the UHF reference tend to show larger errors in ADC oscillator strengths compared to the molecules with lower reference and excited-state SC. To investigate this further, we performed a study of ADC-simulated UV/Vis spectra for the phenyl radical that exhibits large SC in the UHF reference wavefunction. Using the ROHF reference wavefunction improves the agreement of computed spectra with the experiment at the ADC(3) level of theory, but the computed excited states still show significant levels of SC.

Overall, the results of our work suggest that the unrestricted implementations of ADC methods should be used with caution when applied to molecules with the UHF SC > 0.05 a.u. If such calculations need to be performed, we recommend to employ the ROHF reference wavefunction, which allows to reduce SC but does not eliminate it entirely. To address the SC problem, spin-adapted implementations of single-reference ADC methods that preserve spin symmetry for open-shell systems need to be developed.

VI. SUPPLEMENTARY MATERIAL

See the supplementary material for the ADC results computed using the aug-cc-pVDZ basis set, the ADC and LR-CCSDT oscillator strengths, the ADC spectral data for the phenyl radical, and equations for the ADC(2) one- and two-particle reduced density matrices.

VII. ACKNOWLEDGEMENTS

Acknowledgment is made to the donors of the American Chemical Society Petroleum Research Fund for supporting this research (PRF 65903-ND6). Computations were performed at the Ohio Supercomputer Center under projects PAS1963.¹⁵⁹

VIII. DATA AVAILABILITY

The data that supports the findings of this study are available within the article and its supplementary material. Additional data can be made available upon reasonable request.

- ¹G. S. Tyndall, R. A. Cox, C. Granier, R. Lesclaux, G. K. Moortgat, M. J. Pilling, A. R. Ravishankara, and T. J. Wallington, *J. Geophys. Res. Atmos.* **106**, 12157 (2001).
- ²N. Martin, L. Sánchez, M. A. Herranz, B. Illescas, and D. M. Guldi, *Acc. Chem. Res.* **40**, 1015 (2007).
- ³R. Chhantyal-Pun, N. D. Kline, P. S. Thomas, and T. A. Miller, *J. Phys. Chem. Lett.* **1**, 1846 (2010).
- ⁴G.-Y. Liou and P. Storz, *Free Radic. Res.* **44**, 479 (2010).
- ⁵B. Poljsak, U. Glavan, and R. Dahmane, *Int. J. Cancer Res. Prev.* **4**, 193 (2011).
- ⁶B. S. Narendrapurapu, A. C. Simmonett, H. F. Schaefer III, J. A. Miller, and S. J. Klippenstein, *J. Phys. Chem. A* **115**, 14209 (2011).
- ⁷S. Gligorovski, R. Strekowski, S. Barbat, and D. Vione, *Chem. Rev.* **115**, 13051 (2015).
- ⁸H. A. Michelsen, *Proc. Combust. Inst.* **36**, 717 (2017).
- ⁹Y. Li, Z. Cao, and C. Zhu, *AIP Adv.* **8** (2018).
- ¹⁰Y. Li, Y. Gan, and Z. Cao, *J. Comput. Chem.* **40**, 1057 (2019).
- ¹¹K. Wang, L. Huang, N. Eedugurala, S. Zhang, M. A. Sabuj, N. Rai, X. Gu, J. D. Azoulay, and T. N. Ng, *Adv. Energy Mater.* **9**, 1902806 (2019).
- ¹²D. A. Wilcox, V. Agarkar, S. Mukherjee, and B. W. Boudouris, *Annu. Rev. Chem. Biomol. Eng.* **9**, 83 (2018).
- ¹³P. R. Franke, K. B. Moore, H. F. Schaefer, and G. E. Doublerly, *Phys. Chem. Chem. Phys.* **21**, 9747 (2019).
- ¹⁴A. Francés-Monerris, J. Carmona-García, A. U. Acuña, J. Z. Dávalos, C. A. Cuevas, D. E. Kinnison, J. S. Francisco, A. Saiz-López, and D. Roca-Sanjuán, *Angew. Chemie Int. Ed.* **59**, 7605 (2020).
- ¹⁵L. Wang, B. Li, D. D. Dionysiou, B. Chen, J. Yang, and J. Li, *Environ. Sci. Technol.* **56**, 3386 (2022).
- ¹⁶C. D. Sherrill and H. F. Schaefer III, in *Advances in quantum chemistry*, vol. 34 (Elsevier, 1999), pp. 143–269.
- ¹⁷S. Sharma, A. A. Holmes, G. Jeanmairet, A. Alavi, and C. J. Umrigar, *J. Chem. Theory Comput.* **13**, 1595 (2017).
- ¹⁸M. Källay and J. Gauss, *J. Chem. Phys.* **121**, 9257 (2004).
- ¹⁹F. Koskoski and P.-F. Loos, *J. Chem. Theory Comput.* **19**, 2258 (2023).
- ²⁰D. Maurice and M. Head-Gordon, *Int. J. Quantum Chem.* **56**, 361 (1995).
- ²¹M. Head-Gordon, D. Maurice, and M. Oumi, *Chem. Phys. Lett.* **246**, 114 (1995).
- ²²J. Coe and M. J. Paterson, *Int. J. Quantum Chem.* **116**, 1772 (2016).
- ²³D. Maurice and M. Head-Gordon, *J. Phys. Chem.* **100**, 6131 (1996).
- ²⁴M. Roemelt and F. Neese, *J. Phys. Chem. A* **117**, 3069 (2013).
- ²⁵N. C. Handy, J. D. Goddard, and H. F. Schaefer III, *J. Chem. Phys.* **71**, 426 (1979).
- ²⁶T. D. Crawford and H. F. Schaefer, *Rev. Comp. Chem.* **14**, 33 (2000).

- ²⁷I. Shavitt and R. J. Bartlett, *Many-Body Methods in Chemistry and Physics* (Cambridge University Press, Cambridge, UK, 2009).
- ²⁸J. Geertsen, M. Rittby, and R. J. Bartlett, *Chem. Phys. Lett.* **164**, 57 (1989).
- ²⁹D. C. Comeau and R. J. Bartlett, *Chem. Phys. Lett.* **207**, 414 (1993).
- ³⁰J. F. Stanton and R. J. Bartlett, *J. Chem. Phys.* **98**, 7029 (1993).
- ³¹A. I. Krylov, *Annu. Rev. Phys. Chem.* **59**, 433 (2008).
- ³²H. Sekino and R. J. Bartlett, *Int. J. Quant. Chem.* **26**, 255 (1984).
- ³³H. Koch, H. J. A. Jensen, P. Jørgensen, and T. Helgaker, *J. Chem. Phys.* **93**, 3345 (1990).
- ³⁴H. Koch and P. Jørgensen, *J. Chem. Phys.* **93**, 3333 (1990).
- ³⁵G. E. Scuseria and H. F. Schaefer, *Chem. Phys. Lett.* **142**, 354 (1987).
- ³⁶A. I. Krylov, C. D. Sherrill, E. F. Byrd, and M. Head-Gordon, *J. Chem. Phys.* **109**, 10669 (1998).
- ³⁷C. D. Sherrill, A. I. Krylov, E. F. Byrd, and M. Head-Gordon, *J. Chem. Phys.* **109**, 4171 (1998).
- ³⁸R. C. Lochan and M. Head-Gordon, *J. Chem. Phys.* **126**, 164101 (2007).
- ³⁹U. Bozkaya and H. F. Schaefer III, *J. Chem. Phys.* **136**, 204114 (2012).
- ⁴⁰U. Bozkaya and C. D. Sherrill, *J. Chem. Phys.* **139**, 54104 (2013).
- ⁴¹A. V. Copan and A. Y. Sokolov, *J. Chem. Theory Comput.* **14**, 4097 (2018).
- ⁴²F. Koskoski, A. Marie, A. Scemama, M. Caffarel, and P.-F. Loos, *J. Chem. Theory Comput.* **17**, 4756 (2021).
- ⁴³R. J. Buenker and S. D. Peyerimhoff, *Theor. Chim. Acta* **35**, 33 (1974).
- ⁴⁴P. E. M. Siegbahn, *J. Chem. Phys.* **72**, 1647 (1980).
- ⁴⁵P. J. Knowles and H.-J. Werner, *Chem. Phys. Lett.* **115**, 259 (1985).
- ⁴⁶K. Wolinski, H. L. Sellers, and P. Pulay, *Chem. Phys. Lett.* **140**, 225 (1987).
- ⁴⁷D. Mukherjee, R. K. Moitra, and A. Mukhopadhyay, *Mol. Phys.* **33**, 955 (1977).
- ⁴⁸B. Jeziorski and H. J. Monkhorst, *Physical Review A* **24**, 1668 (1981).
- ⁴⁹H.-J. Werner and P. J. Knowles, *J. Chem. Phys.* **89**, 5803 (1988).
- ⁵⁰U. S. Mahapatra, B. Datta, and D. Mukherjee, *Mol. Phys.* **94**, 157 (1998).
- ⁵¹J. Pittner, *J. Chem. Phys.* **118**, 10876 (2003).
- ⁵²F. A. Evangelista, W. D. Allen, and H. F. Schaefer, *J. Chem. Phys.* **127**, 024102 (2007).
- ⁵³D. Datta, L. Kong, and M. Nooijen, *J. Chem. Phys.* **134**, 214116 (2011).
- ⁵⁴D. Datta and M. Nooijen, *J. Chem. Phys.* **137**, 204107 (2012).
- ⁵⁵F. A. Evangelista and J. Gauss, *J. Chem. Phys.* **134**, 114102 (2011).
- ⁵⁶A. Köhn, M. Hanauer, L. A. Mück, T.-C. Jagau, and J. Gauss, *Wiley Interdiscip. Rev. Comput. Mol. Sci.* **3**, 176 (2013).
- ⁵⁷M. Nooijen, O. Demel, D. Datta, L. Kong, K. R. Shamasundar, V. Lotrich, L. M. Huntington, and F. Neese, *J. Chem. Phys.* **140**, 081102 (2014).
- ⁵⁸P. K. Samanta, D. Mukherjee, M. Hanauer, and A. Köhn, *J. Chem. Phys.* **140**, 134108 (2014).
- ⁵⁹Y. A. Aoto and A. Köhn, *J. Chem. Phys.* **144**, 074103 (2016).
- ⁶⁰A. Montoya, T. N. Truong, and A. F. Sarofim, *J. Phys. Chem. A* **104**, 6108 (2000).
- ⁶¹P. G. Szalay and J. Gauss, *J. Chem. Phys.* **112**, 4027 (2000).
- ⁶²A. I. Krylov, *Rev. Comput. Chem.* **30**, 151 (2017).
- ⁶³A. S. Menon and L. Radom, *J. Phys. Chem. A* **112**, 13225 (2008).
- ⁶⁴A. Ipatov, F. Cordova, L. J. Doriol, and M. E. Casida, *J. Mol. Struct. THEOCHEM* **914**, 60 (2009).
- ⁶⁵X. Zhang and J. M. Herbert, *J. Chem. Phys.* **143** (2015).
- ⁶⁶M.-P. Kitsaras and S. Stopkowicz, *J. Chem. Phys.* **154**, 131101 (2021).
- ⁶⁷J. Schirmer, *Phys. Rev. A* **26**, 2395 (1982).
- ⁶⁸J. Schirmer, *Phys. Rev. A* **43**, 4647 (1991).
- ⁶⁹A. B. Trofimov and J. Schirmer, *J. Phys. B At. Mol. Opt. Phys.* **28**, 2299 (1995).
- ⁷⁰F. Mertins and J. Schirmer, *Phys. Rev. A* **53**, 2140 (1996).
- ⁷¹A. B. Trofimov, G. Stelter, and J. Schirmer, *J. Chem. Phys.* **111**, 9982 (1999).
- ⁷²J. Schirmer and A. B. Trofimov, *J. Chem. Phys.* **120**, 11449 (2004).
- ⁷³A. Dreuw and M. Wormit, *WIREs Comput. Mol. Sci.* **5**, 82 (2014).
- ⁷⁴A. Y. Sokolov, *J. Chem. Phys.* **149**, 204113 (2018).
- ⁷⁵J. H. Starcke, M. Wormit, and A. Dreuw, *J. Chem. Phys.* **130** (2009).
- ⁷⁶B. Lunkenheimer and A. Köhn, *J. Chem. Theory Comput.* **9**, 977 (2013).
- ⁷⁷P. H. P. Harbach, M. Wormit, and A. Dreuw, *J. Chem. Phys.* **141** (2014).
- ⁷⁸R. Sarkar, M.-C. Heitz, G. Royal, and M. Boggio-Pasqua, *J. Phys. Chem. A* **124**, 1567 (2020).
- ⁷⁹N. G. Wong, C. D. Rankine, and C. E. Dessent, *J. Phys. Chem. A* **125**, 6703 (2021).
- ⁸⁰N. O. Winter, N. K. Graf, S. Leutwyler, and C. Hättig, *Phys. Chem. Chem. Phys.* **15**, 6623 (2013).
- ⁸¹H. Li, R. Nieman, A. J. A. Aquino, H. Lischka, and S. Tretiak, *J. Chem. Theory Comput.* **10**, 3280 (2014).
- ⁸²A. N. Panda, F. Plasser, A. J. Aquino, I. Burghardt, and H. Lischka, *J. Phys. Chem. A* **117**, 2181 (2013).
- ⁸³F. Plasser and H. Lischka, *J. Chem. Theory Comput.* **8**, 2777 (2012).
- ⁸⁴A. J. Aquino, D. Nachtigallova, P. Hobza, D. G. Truhlar, C. Hättig, and H. Lischka, *J. Comput. Chem.* **32**, 1217 (2011).
- ⁸⁵S. Höfener, B. A. Günther, M. E. Harding, and L. H. Gade, *J. Phys. Chem. A* **123**, 3160 (2019).
- ⁸⁶A. B. Trofimov, G. Stelter, and J. Schirmer, *J. Chem. Phys.* **117**, 6402 (2002).
- ⁸⁷A. Dreuw and M. Wormit, *Wiley Interdiscip. Rev. Comput. Mol. Sci.* **5**, 82 (2015).
- ⁸⁸R. Maier, M. Bauer, and A. Dreuw, *J. Chem. Phys.* **159** (2023).
- ⁸⁹J. Leitner, A. L. Dempwolff, and A. Dreuw, *J. Chem. Phys.* **157** (2022).
- ⁹⁰D. Lefrancois, M. Wormit, and A. Dreuw, *J. Chem. Phys.* **143** (2015).
- ⁹¹G. P. Paran, C. Utku, and T.-C. Jagau, *Phys. Chem. Chem. Phys.* **24**, 27146 (2022).
- ⁹²T. L. Stahl, S. Banerjee, and A. Y. Sokolov, *J. Chem. Phys.* **157** (2022).
- ⁹³G. Csanak, H. S. Taylor, and R. Yaris, in *Adv. At. Mol. Phys.*, vol. 7 (Elsevier, 1971), pp. 287–361.
- ⁹⁴A. L. Fetter and J. D. Walecka, *Quantum theory of many-particle systems* (Dover Publications, 2003).
- ⁹⁵W. H. Dickhoff and D. Van Neck, *Many-body theory exposed!: propagator description of quantum mechanics in many-body systems* (World Scientific Publishing Co., 2005).
- ⁹⁶D. Danovich, *Wiley Interdiscip. Rev. Comput. Mol. Sci.* **1**, 377 (2011).
- ⁹⁷C. Möller and M. S. Plesset, *Phys. Rev.* **46**, 618 (1934).
- ⁹⁸I. M. Mazin and A. Y. Sokolov, *J. Chem. Theory Comput.* **17**, 6152 (2021).
- ⁹⁹M. D. Prasad, S. Pal, and D. Mukherjee, *Phys. Rev. A* **31**, 1287 (1985).
- ¹⁰⁰D. Mukherjee and W. Kutzelnigg, in *Many-Body Methods in Quantum Chemistry* (Springer, Berlin, Heidelberg, Berlin, Heidelberg, 1989), pp. 257–274.
- ¹⁰¹S. Banerjee and A. Y. Sokolov, *J. Chem. Phys.* **151**, 224112 (2019).
- ¹⁰²D. Stück and M. Head-Gordon, *J. Chem. Phys.* **139**, 244109 (2013).

- ¹⁰³J. S. Andrews, D. Jayatilaka, R. G. A. Bone, N. C. Handy, and R. D. Amos, *Chem. Phys. Lett.* **183**, 423 (1991).
- ¹⁰⁴J. Kouba and Y. Öhrn, *Int. J. Quantum Chem.* **3**, 513 (1969).
- ¹⁰⁵G. D. Purvis, H. Sekino, and R. J. Bartlett, *Collect. Czechoslov. Chem. Commun.* **53**, 2203 (1988).
- ¹⁰⁶J. F. Stanton, *J. Chem. Phys.* **101**, 371 (1994).
- ¹⁰⁷A. I. Krylov, *J. Chem. Phys.* **113**, 6052 (2000).
- ¹⁰⁸A. B. Trofimov and J. Schirmer, *J. Chem. Phys.* **123**, 144115 (2005).
- ¹⁰⁹S. Knippenberg, D. R. Rehn, M. Wormit, J. H. Starcke, I. L. Rusakova, A. B. Trofimov, and A. Dreuw, *J. Chem. Phys.* **136**, 64107 (2012).
- ¹¹⁰F. Plasser, M. Wormit, and A. Dreuw, *J. Chem. Phys.* **141**, 24106 (2014).
- ¹¹¹F. Plasser, S. A. Bäppler, M. Wormit, and A. Dreuw, *J. Chem. Phys.* **141**, 24107 (2014).
- ¹¹²A. L. Dempwolff, A. C. Paul, A. M. Belogolova, A. B. Trofimov, and A. Dreuw, *J. Chem. Phys.* **152**, 024113 (2020).
- ¹¹³A. L. Dempwolff, A. M. Belogolova, A. B. Trofimov, and A. Dreuw, *J. Chem. Phys.* **154**, 104117 (2021).
- ¹¹⁴Q. Sun, X. Zhang, S. Banerjee, P. Bao, M. Barbry, N. S. Blunt, N. A. Bogdanov, G. H. Booth, J. Chen, Z.-H. Cui, and Others, *J. Chem. Phys.* **153**, 24109 (2020).
- ¹¹⁵J. L. Whitten, *J. Chem. Phys.* **58**, 4496 (1973).
- ¹¹⁶O. Vahtras, J. Almlöf, and M. Feyereisen, *Chem. Phys. Lett.* **213**, 514 (1993).
- ¹¹⁷M. Feyereisen, G. Fitzgerald, and A. Komornicki, *Chem. Phys. Lett.* **208**, 359 (1993).
- ¹¹⁸B. I. Dunlap, J. Connolly, and J. Sabin, *J. Chem. Phys.* **71**, 3396 (1979).
- ¹¹⁹P.-F. Loos, A. Scemama, M. Boggio-Pasqua, and D. Jacquemin, *J. Chem. Theory Comput.* **16**, 3720 (2020).
- ¹²⁰T. H. Dunning Jr., *J. Chem. Phys.* **90**, 1007 (1989).
- ¹²¹R. A. Kendall, T. H. Dunning Jr., and R. J. Harrison, *J. Chem. Phys.* **96**, 6796 (1992).
- ¹²²B. P. Prascher, D. E. Woon, K. A. Peterson, T. H. Dunning, and A. K. Wilson, *Theor. Chem. Acc.* **128**, 69 (2011).
- ¹²³D. E. Woon and T. H. Dunning Jr., *J. Chem. Phys.* **98**, 1358 (1993).
- ¹²⁴C. Hättig, *Phys. Chem. Chem. Phys.* **7**, 59 (2005).
- ¹²⁵F. Weigend, A. Köhn, and C. Hättig, *J. Chem. Phys.* **116**, 3175 (2002).
- ¹²⁶M. Kállay, P. R. Nagy, D. Mester, Z. Rolik, G. Samu, J. Csontos, J. Csóka, P. B. Szabó, L. Gyevi-Nagy, B. Hégly, and Others, *J. Chem. Phys.* **152** (2020).
- ¹²⁷M. Kállay, P. R. Nagy, D. Mester, L. Gyevi-Nagy, J. Csóka, P. B. Szabó, Z. Rolik, G. Samu, J. Csontos, B. Hégly, Á. Ganyecz, I. Ladjánszki, L. Szegedy, B. Ladóczki, K. Petrov, M. Farkas, P. D. Mezei, and R. A. Horváth, MRCC, a quantum chemical program suite, \url{http://www.mrcc.hu}.
- ¹²⁸E. Epifanovsky, A. T. B. Gilbert, X. Feng, J. Lee, Y. Mao, N. Mardirossian, P. Pokhilko, A. F. White, M. P. Coons, A. L. Dempwolff, and Others, *J. Chem. Phys.* **155**, 84801 (2021).
- ¹²⁹D. Jacquemin, I. Duchemin, A. Blondel, and X. Blase, *J. Chem. Theory Comput.* **12**, 3969 (2016).
- ¹³⁰A. Chrayteh, A. Blondel, P.-F. Loos, and D. Jacquemin, *J. Chem. Theory Comput.* **17**, 416 (2020).
- ¹³¹R. Sarkar, M. Boggio-Pasqua, P.-F. Loos, and D. Jacquemin, *J. Chem. Theory Comput.* **17**, 1117 (2021).
- ¹³²Y. Damour, R. Quintero-Monsebaiz, M. Caffarel, D. Jacquemin, F. Koskoski, A. Scemama, and P.-F. Loos, *J. Chem. Theory Comput.* **19**, 221 (2022).
- ¹³³M. Wormit, D. R. Rehn, P. H. P. Harbach, J. Wenzel, C. M. Krauter, E. Epifanovsky, and A. Dreuw, *Mol. Phys.* **112**, 774 (2014).
- ¹³⁴M. Schütz, *J. Chem. Phys.* **142** (2015).
- ¹³⁵V. B. O'Donnell, G. C. Smith, and O. T. Jones, *Mol. Pharmacol.* **46**, 778 (1994).
- ¹³⁶H. Imoto, N. Sasaki, M. Iwase, U. Nakamura, M. Oku, K. Sonoki, Y. Uchizono, and M. Iida, *Endocrinology* **149**, 5391 (2008).
- ¹³⁷Y. Sekine, S. Lebonnois, H. Imanaka, T. Matsui, E. L. O. Bakes, C. P. McKay, B. N. Khare, and S. Sugita, *Icarus* **194**, 201 (2008).
- ¹³⁸M. Frenklach and E. D. Feigelson, *Astrophys. Journal, Part 1 (ISSN 0004-637X)*, vol. 341, June 1, 1989, p. 372-384. **341**, 372 (1989).
- ¹³⁹X. Gu and R. I. Kaiser, *Acc. Chem. Res.* **42**, 290 (2009).
- ¹⁴⁰B. M. Jones, F. Zhang, R. I. Kaiser, A. Jamal, A. M. Mebel, M. A. Cordiner, and S. B. Charnley, *Proc. Natl. Acad. Sci.* **108**, 452 (2011).
- ¹⁴¹R. I. Kaiser, D. S. N. Parker, and A. M. Mebel, *Annu. Rev. Phys. Chem.* **66**, 43 (2015).
- ¹⁴²D. S. N. Parker and R. I. Kaiser, *Chem. Soc. Rev.* **46**, 452 (2017).
- ¹⁴³O. Martinez Jr., K. N. Crabtree, C. A. Gottlieb, J. F. Stanton, and M. C. McCarthy, *Angew. Chemie* **127**, 1828 (2015).
- ¹⁴⁴G. Blanquart, *Int. J. Quantum Chem.* **115**, 796 (2015).
- ¹⁴⁵G. Porter and B. Ward, *Proc. R. Soc. London. Ser. A. Math. Phys. Sci.* **287**, 457 (1965).
- ¹⁴⁶B. Cercek and M. Kongshaug, *J. Phys. Chem.* **74**, 4319 (1970).
- ¹⁴⁷J. H. Miller, L. Andrews, P. A. Lund, and P. N. Schatz, *J. Chem. Phys.* **73**, 4932 (1980).
- ¹⁴⁸N. Ikeda, N. Nakashima, and K. Yoshihara, *J. Am. Chem. Soc.* **107**, 3381 (1985).
- ¹⁴⁹W. G. Hatton, N. P. Hacker, and P. H. Kasai, *J. Chem. Soc. Chem. Commun.* pp. 227–229 (1990).
- ¹⁵⁰J. M. Engert and B. Dick, *Appl. Phys. B* **63**, 531 (1996).
- ¹⁵¹K. Tonokura, Y. Norikane, M. Koshi, Y. Nakano, S. Nakamichi, M. Goto, S. Hashimoto, M. Kawasaki, M. P. Sulbaek Andersen, M. D. Hurley, and Others, *J. Phys. Chem. A* **106**, 5908 (2002).
- ¹⁵²Y. Song, M. Lucas, M. Alcaraz, J. Zhang, and C. Brazier, *J. Chem. Phys.* **136** (2012).
- ¹⁵³J. G. Radziszewski, *Chem. Phys. Lett.* **301**, 565 (1999).
- ¹⁵⁴J. Pacansky and D. W. Brown, *J. Phys. Chem.* **87**, 1553 (1983).
- ¹⁵⁵R. P. Johnson, *J. Org. Chem.* **49**, 4857 (1984).
- ¹⁵⁶M. Krauss and S. Roszak, *J. Mol. Struct. THEOCHEM* **310**, 155 (1994).
- ¹⁵⁷G.-S. Kim, A. M. Mebel, and S. H. Lin, *Chem. Phys. Lett.* **361**, 421 (2002).
- ¹⁵⁸M. Biczysko, J. Bloino, and V. Barone, *Chem. Phys. Lett.* **471**, 143 (2009).
- ¹⁵⁹Ohio Supercomputer Center, Technical report (1987).